



## Chemical calcium indicators

R. Madelaine Paredes<sup>1</sup>, Julie C. Etzler<sup>1</sup>, Lora Talley Watts, Wei Zheng, James D. Lechleiter\*

Department of Cellular and Structural Biology, University of Texas Health Science Center at San Antonio, 7703 Floyd Curl Drive, San Antonio, TX 78229, USA

### ARTICLE INFO

#### Article history:

Accepted 12 September 2008

Available online 16 October 2008

#### Keywords:

Chemical calcium indicators

Microscopy

### ABSTRACT

Our understanding of the underlying mechanisms of  $\text{Ca}^{2+}$  signaling as well as our appreciation for its ubiquitous role in cellular processes has been rapidly advanced, in large part, due to the development of fluorescent  $\text{Ca}^{2+}$  indicators. In this chapter, we discuss some of the most common chemical  $\text{Ca}^{2+}$  indicators that are widely used for the investigation of intracellular  $\text{Ca}^{2+}$  signaling. Advantages, limitations and relevant procedures will be presented for each dye including their spectral qualities, dissociation constants, chemical forms, loading methods and equipment for optimal imaging. Chemical indicators now available allow for intracellular  $\text{Ca}^{2+}$  detection over a very large range (<50 nM to >50  $\mu\text{M}$ ). High affinity indicators can be used to quantify  $\text{Ca}^{2+}$  levels in the cytosol while lower affinity indicators can be optimized for measuring  $\text{Ca}^{2+}$  in subcellular compartments with higher concentrations. Indicators can be classified into either single wavelength or ratiometric dyes. Both classes require specific lasers, filters, and/or detection methods that are dependent upon their spectral properties and both classes have advantages and limitations. Single wavelength indicators are generally very bright and optimal for  $\text{Ca}^{2+}$  detection when more than one fluorophore is being imaged. Ratiometric indicators can be calibrated very precisely and they minimize the most common problems associated with chemical  $\text{Ca}^{2+}$  indicators including uneven dye loading, leakage, photobleaching, and changes in cell volume. Recent technical advances that permit *in vivo*  $\text{Ca}^{2+}$  measurements will also be discussed.

© 2008 Elsevier Inc. All rights reserved.

### 1. Introduction

Intracellular  $\text{Ca}^{2+}$  is central to a multitude of physiological processes ranging from neuronal signaling and exocytosis to muscle contraction and bone formation [1]. Abnormalities in  $\text{Ca}^{2+}$ -signaling have severe pathological consequences and can result in neurodegeneration [2–4], disorders of the central nervous system, skeletal muscle defects [5,6], heart disease [7,8], and skin disorders [9] among others [10]. A very successful approach to studying the role of  $\text{Ca}^{2+}$  in a specific cellular process has been the use of fluorescent  $\text{Ca}^{2+}$  indicators. Broadly speaking, these indicators exhibit altered fluorescent properties when bound with  $\text{Ca}^{2+}$ . There are generally two classes of  $\text{Ca}^{2+}$  indicators: genetically encoded fluorescent proteins and chemically engineered fluorophores. The focus of this review will be on the most commonly used chemical indicators that have been optimized for the investigation of cytosolic and organelle associated  $\text{Ca}^{2+}$ .

$\text{Ca}^{2+}$  indicators bind and interact only with freely diffusible  $\text{Ca}^{2+}$  ions. In this light, it is important to remember that the majority of  $\text{Ca}^{2+}$  within cells is not free to diffuse but tightly bound to various cellular buffers. The ratio of bound to free  $\text{Ca}^{2+}$  varies from cell to cell as well as within the various compartments of the cell. In very

general terms, cytosolic  $\text{Ca}^{2+}$  is buffered 100 to 1, meaning that for every 100  $\text{Ca}^{2+}$  ions in the cytosol, only 1 ion is free to diffuse. The bound to free ratio of  $\text{Ca}^{2+}$  within the endoplasmic reticulum is of the order of 10 to 1 [11–13]. Chemical  $\text{Ca}^{2+}$  indicators themselves also act as  $\text{Ca}^{2+}$  buffers and can therefore impact both the levels and most noticeably, the kinetics of  $\text{Ca}^{2+}$ -signaling within cells. It is for these reasons that users must carefully consider not only the spectral characteristics of a chemical indicator (e.g. whether it fluoresces in the red or green spectrum), but also pay close attention to its binding properties. For example, is the binding affinity appropriate for the cellular compartment or physiological process that you are studying? Each of these concerns will be addressed below. Utilization of chemical  $\text{Ca}^{2+}$  indicators will be discussed in terms of their specific properties, binding affinities, advantages and limitations when measuring intracellular  $\text{Ca}^{2+}$  both *in vitro* as well as for *in vivo* measurements.

### 2. Chemical vs. genetically encoded $\text{Ca}^{2+}$ indicators

A major advantage of chemical indicators over genetically encoded fluorescent proteins is the broad range of  $\text{Ca}^{2+}$  affinities that are commercially available for the user as well as the ease of introducing and rapidly utilizing these dyes for experiments. Chemical  $\text{Ca}^{2+}$  indicators do not have to be transfected or expressed in cells. Cell-loading protocols for chemical  $\text{Ca}^{2+}$  indicators

\* Corresponding author. Fax: +1 210 567 6781.

E-mail address: [lechleiter@uthscsa.edu](mailto:lechleiter@uthscsa.edu) (J.D. Lechleiter).

<sup>1</sup> These authors contributed equally.

have been very well-established [14,15]. A major disadvantage is that the cellular localization of  $\text{Ca}^{2+}$  indicators cannot be easily controlled or specifically targeted to a particular organelle. In addition, chemical indicators tend to compartmentalize and are eventually extruded from the cell during long recording experiments [16,17]. A relatively simple and successful strategy to combat the problem of compartmentalization has been to generate indicators with a large dextran tag [18–20]. This strategy permits  $\text{Ca}^{2+}$  levels to be recorded for long extended periods, up to days at a time [21]. However, a limitation of dextran tagged dyes is that they are more difficult to load and generally need to be directly injected into cells.

### 3. Selection criteria of chemical $\text{Ca}^{2+}$ indicators

There are multiple considerations when selecting the most appropriate  $\text{Ca}^{2+}$  indicator for your experiments. When properly calibrated, different indicators can reasonably be expected to give similar results for the same experiment. However,  $\text{Ca}^{2+}$  indicators are by definition,  $\text{Ca}^{2+}$  buffers that can significantly affect physiological signaling. The user must frequently balance the desire to increase the strength of indicator signal with the problems associated with increasing an indicator's concentration. On occasion, it is possible to work with an indicator with a lower  $\text{Ca}^{2+}$  affinity. This can reduce the impact of buffering but frequently is done so at the cost of limiting the signal strength. When working with multiple fluorophores or endogenous autofluorescence, it may be necessary to choose an indicator based primarily on its spectral properties. Alternatively, your imaging system may be limited by the availability of various excitation wavelengths from which to choose. In the following section, we discuss the primary criteria that can be considered to help choose the most appropriate  $\text{Ca}^{2+}$  indicator.

#### 3.1. $\text{Ca}^{2+}$ affinities of indicator dyes

The dissociation constant ( $K_d$ ) [22] or its inverse, the association constant ( $K_a$ ), describes how tightly an indicator dye binds  $\text{Ca}^{2+}$  ions. The  $K_d$  has molar units and corresponds to the concentration of  $\text{Ca}^{2+}$  at which half the indicator molecules are bound with  $\text{Ca}^{2+}$  at equilibrium. When possible, indicators should be utilized to measure  $\text{Ca}^{2+}$  concentrations between 0.1 and 10 times their  $K_d$ . This is the range over which  $\text{Ca}^{2+}$ -dependent changes in fluorescence are the largest. Of the indicator dyes that are now commercially available, intracellular  $\text{Ca}^{2+}$  can be measured in compartments with levels less than 50 nM to regions greater than 50  $\mu\text{M}$ . It is important to note that the  $K_d$  is dependent on pH, temperature, viscosity, ionic strength, protein binding and the amount of  $\text{Mg}^{2+}$  and other ions present [23–26]. Consequently, the  $K_d$  of a specific indicator dye *in vitro* may not have the same value as the  $K_d$  *in vivo*. For an accurate calibration of  $\text{Ca}^{2+}$  levels, it is necessary to empirically measure the  $K_d$  *in situ*, not only for a specific cell type, but also for each subcellular compartment.

Another consideration when choosing indicator dyes is that  $\text{Ca}^{2+}$  signals are generally transient in nature and hence, are mea-

sured under non-equilibrium conditions. Consequently, it is sometimes necessary to be aware of the speed with which an indicator dye binds  $\text{Ca}^{2+}$ . The  $K_a$  (as opposed to its inverse, the  $K_d$ ) is used to describe these binding characteristics. The  $K_a$  is defined as the ratio of the  $\text{Ca}^{2+}$  binding rate ( $K_{\text{on}}$  in units of  $\text{M}^{-1} \text{s}^{-1}$ ) over the  $\text{Ca}^{2+}$  dissociation rate ( $K_{\text{off}}$ , in units of  $\text{s}^{-1}$ ). A time constant ( $\tau$ ) for equilibrium binding to occur can also be defined as:

$$1/\tau = K_{\text{on}}[\text{Buffer}_{\text{total}}], \quad (1)$$

assuming a 1:1 reaction:



Equilibrium affinities and binding rate constants for some commonly used  $\text{Ca}^{2+}$  indicator dyes are presented in Table 1.

#### 3.2. Spectral properties of indicator dyes

In addition to the strength and speed of  $\text{Ca}^{2+}$ -binding to a particular dye, the  $\text{Ca}^{2+}$ -dependent spectral changes that occur must be carefully considered.  $\text{Ca}^{2+}$  dyes can be categorized as either ratiometric or single wavelength indicators. Single wavelength indicators exhibit significant  $\text{Ca}^{2+}$  dependent changes in fluorescence intensity without shifting their excitation or emission wavelengths. It is easier to avoid or minimize spectral overlap with other fluorophores when working with single wavelength indicators [32–36]. Ratiometric indicators shift the peak wavelength of either their excitation or emission curve upon binding  $\text{Ca}^{2+}$ . This class of indicators permits a very accurate quantification of  $\text{Ca}^{2+}$  concentration that is corrected for uneven dye loading, dye leakage, photobleaching and changes in cell volume, but at the cost of increased spectral bandwidth. Calibration of  $\text{Ca}^{2+}$  signals for both single wavelength and ratiometric dyes will be discussed below.

Imaging equipment can also limit the specific dyes that can be utilized. For example, the number of excitation wavelengths that can be used in single photon laser scanning microscopes is determined by the specific lasers that are available. For conventional wide-field epi-fluorescent microscopes, the excitation of  $\text{Ca}^{2+}$  indicators is generally limited only by the availability of an appropriate filter set. The two most common lamp sources in use in wide-field epi-fluorescence are the Mercury Arc and Xenon burners. Both light sources are broad-spectrum emitters. However, Mercury lamps do not provide an even intensity across the entire spectrum. The highest intensity peaks occur at 334, 365, 406, 435, 546 and 578 nm with steady lower intensity at wavelengths in between these values. Xenon lamps have a relatively even intensity across the visible spectrum, but they are not as intense and are particularly lower in the ultraviolet. When working with two-photon laser scanning microscopes, the absorption properties of  $\text{Ca}^{2+}$  dyes can be significantly different than what might be predicted based on doubling the peak single photon absorption wavelength. Additional absorption peaks are frequently present at shorter wavelengths. Absorption curves can also be much broader for two-photon excitation, making it more difficult to exclusively

**Table 1**  
Equilibrium affinities and binding rate constants of  $\text{Ca}^{2+}$  indicator dyes.

$\text{Ca}^{2+}$ dye	$K_{\text{on}}, \text{Ca}^{2+}$ ( $\times 10^7 \text{M}^{-1} \text{s}^{-1}$ )	$K_{\text{off}}, \text{Ca}^{2+}$ ( $\text{s}^{-1}$ )	$\tau$ equilibrium ( $\mu\text{s}$ )	$K_d, \text{Ca}^{2+}$ ( $\mu\text{M}$ )	$K_d, \text{Mg}^{2+}$ (mM)	Reference
Fura-2	15	23	6.7	0.23 (0.14)	—	[27–29]
Magnesium Green NTA	9	1750	11	19 (6)	2.4 (1.0)	[30,31]
Furaptra	5.0	5000	20	100 (17)	5.3 (2.5)	[30,31]
Mag-Fura-Red	2.1	5000	—	17	2.5	[31]

The time constant ( $\tau$ ) for buffer/calcium equilibrium is defined as:  $1/\tau = K_{\text{on}}[\text{Buffer}_{\text{total}}]$  assuming a 1 mM Buffer concentration and a 1:1 reaction as described in the text. When available, *in situ* cytoplasmic values are reported with the corresponding *in vitro* estimates given in parenthesis. Note that the  $K_{\text{on}}$  values greater than  $10 \times 10^7 \text{M}^{-1} \text{s}^{-1}$  are diffusion limited [31].

**Table 2**  
High affinity calcium indicators.

Indicator	$K_d$ for $\text{Ca}^{2+}$ (nM)	Excitation (nm), emission (nm)	Notes	Reference
Calcium Green-1	190	490 ex, 531 em	Single wavelength	[39,40]
Fluo-3	325	506 ex, 526 em	Single wavelength	[41,42]
Fluo-4	345	494 ex, 516 em	Single wavelength	[43–45]
Fura-2	145	363/335 ex, 512 em	Dual excitation/single emission	[39,46,47]
Indo-1	230	488 ex, 405/485 em	Single excitation/dual emission	[47]
Oregon Green 488 Bapta-1	170	488 ex, 520 em	Single long wavelength	[48]
Fura-4F	0.77	336/366 ex, 511 em	Ratiometric excitation/single emission	[49]
Fura-5F	0.40	336/363 ex, 512 em	Ratiometric excitation/single emission	[50]
Calcium Crimson	185	590 ex, 615 em	Single long wavelength	[39]
X-Rhod-1	0.7	580 ex, 602 em	Single excitation/emission	[51,52]

excite a dye at a single wavelength. Finally, absorption is sometimes less efficient, making  $\text{Ca}^{2+}$ -dependent changes in fluorescent signals less intense. The excitation/emission spectral properties of the most commonly used  $\text{Ca}^{2+}$  indicator dyes for both single photon and two-photon excitation are presented in Tables 2 and 3 based on whether they are high or low affinity indicators.

### 3.3. $\text{Ca}^{2+}$ dye indicator forms

$\text{Ca}^{2+}$  indicator dyes are commercially available in three chemical forms: salts, dextran conjugates or acetoxymethyl (AM) esters. Salts are the simplest form of  $\text{Ca}^{2+}$  indicators, but because of their hydrophilic nature, they are membrane impermeable and require invasive loading procedures. They can be introduced into cells by multiple techniques including microinjection, diffusion from patch clamp pipettes, electroporation and lipotransfer using liposomes. Once introduced into the cell, the salt form of  $\text{Ca}^{2+}$  indicators rapidly equilibrates and can be used for  $\text{Ca}^{2+}$ -imaging measurements within minutes. However, it was recognized early on that once introduced into the cytoplasm,  $\text{Ca}^{2+}$  dyes begin to compartmentalize into membrane bound vacuoles. Compartmentalization of the indicator dyes degrades  $\text{Ca}^{2+}$  measurements within the cytosol, but is generally not a major problem for short-term recordings performed within 30 min to an hour. The acceptable period for  $\text{Ca}^{2+}$ -imaging measurements depends on both the cell type and temperature and in the end, needs to be empirically determined. Dextran conjugates of  $\text{Ca}^{2+}$  indicator dyes were specifically engineered to address the problem of compartmentalization. Dextrans have high water solubility, low toxicity, and exhibit essentially no compartmentalization over very long recording periods up to days in length. Dextran conjugates are available for all of the most common and popular  $\text{Ca}^{2+}$  indicators including, Fluo-4, Rhod-2, Fura-2, and Oregon Green 488 BAPTA-1. The only caveat of using dextran

conjugated  $\text{Ca}^{2+}$  dyes is that like the salt form, these indicators are membrane impermeable and must be invasively introduced into the cell. One technique for loading dextran conjugates is to use pinocytotic cell-loading reagent, created by Molecular Probes which allows the indicator to be taken up by the cell into pinocytotic vesicles which can be lysed when the cells are put into hypotonic medium [37].

$\text{Ca}^{2+}$  indicator dyes were engineered with AM esters to offer a more convenient method for loading hydrophilic dyes into cells. AM dyes are sufficiently hydrophobic in that they are membrane permeable and can be passively loaded into cells simply by adding them to the extracellular medium. Intracellular esterases then cleave the AM group and trap the dye inside cells. This method of dye loading also effectively concentrates  $\text{Ca}^{2+}$  indicators inside cells such that a bath concentration of 1–5  $\mu\text{M}$  results in a cytosolic concentration of greater than 100  $\mu\text{M}$ . Another advantage of using AM-linked  $\text{Ca}^{2+}$  dyes is that subcellular compartments can be labeled. For example, low affinity  $\text{Ca}^{2+}$  indicators can be used to monitor  $\text{Ca}^{2+}$  levels in the endoplasmic reticulum as discussed below. Recommended procedures to dissolve dyes and optimize cellular or subcellular loading are provided in the manufacturer's product sheet. In general, dimethylsulfoxide (DMSO) is used to initially dissolve AM-linked  $\text{Ca}^{2+}$  dyes followed by serial dilutions in the appropriate extracellular media. An advantage of DMSO is that it inhibits or slows the hydrolysis of esters in moist environments. This helps to preserve the activity of the indicator until it is in the cytosol. Pluronic-F127 is also used to help disperse the AM-linked indicator dyes into medium given the fact that AM groups have low solubility in aqueous solutions [14,15,38].

There are several commercial sources where researchers typically purchase  $\text{Ca}^{2+}$  indicator dyes. These include Molecular Probes <http://probes.invitrogen.com/handbook/tables/0355.html>, Teflabs <http://www.teflabs.com/>, ALEXIS Biochemical's (<http://www.alexis-bio.com/>)

**Table 3**  
Low Affinity  $\text{Ca}^{2+}$  indicators.

Indicator	$K_d$ for $\text{Mg}^{2+}$ (mM)	$K_d$ for $\text{Ca}^{2+}$ ( $\mu\text{M}$ )	Excitation (nm), emission (nm)	Notes	Reference
Mag-Fura-2	1.9	25	329/369 ex, 511em	Ratiometric excitation/single emission	[60,71,72]
Mag-Fluo-4	4.7	22	490 ex, 517 em	Single excitation/emission	[73]
Mag-Indo-1	2.7	35	349 ex, 480/390 em	Single excitation/ratiometric emission	[74]
Mag-Fura-5	2.3	28	369 ex, 505 em	Ratiometric excitation/single emission	[75]
Mag-Fura-Red	2.5	17	488 ex, 630 em	Ratiometric excitation/single emission	[76]
Fura-2-ff	—	35	335/360 ex, 505 em	Ratiometric excitation/single emission	[77,78]
Fluo-5 N	—	90	491 ex, 516 em	Single excitation/emission	[17,79]
Oregon Green BAPTA-5N	—	20	494 ex, 521 em	Single excitation/emission	[80]
Fura-6F	—	5.3	336/364 ex, 512em	Ratiometric excitation/single emission	[49,81]
Fura-FF	—	5.5	335/364 ex, 510em	Ratiometric excitation/single emission	[49,82,83]
Fluo 5 F	—	2.3	491 ex, 518 em	Single excitation/emission	[84,85]
Fluo 4FF	—	9.7	491 ex, 516 em	Single excitation/emission	[86,87]
Oregon Green 488 BAPTA-6F	—	3	494 ex, 524 em	Single excitation/emission	[88,89]
Rhod-FF	—	19	552 ex, 580 em	Single excitation/emission	[90,91]
X-Rhod-5F	—	1.6	581 ex, 603 em	Single excitation/emission	[52,92]
X-Rhod-FF	—	17	580 ex, 603 em	Single excitation/emission	[53]

[www.alexis-biochemicals.com](http://www.alexis-biochemicals.com)) part of AXORA (<http://www.axora.com>) and Anaspec (<http://www.anaspec.com/>).

#### 4. High affinity Ca<sup>2+</sup> indicators

This class of indicators is the most commonly used by investigators to measure Ca<sup>2+</sup>. In general, they are well characterized and come in a sufficient array of spectral properties and binding affinities that can be utilized to suit the needs of most experiments. The general characteristics of each dye are presented in Table 2. Below, we discuss some of the caveats that are specific to each dye.

Table 2 is based on product data manuals by Molecular Probes revised in June of 2005, and other published papers.

##### 4.1. Calcium Green-1

This Ca<sup>2+</sup> indicator has a high quantum yield, low photo toxicity and can be imaged on virtually all fluorescent microscopes given that its peak excitation (~490 nm) and peak emission (~530 nm) are similar to standard fluorescein dyes. Its Ca<sup>2+</sup> affinity ( $K_d$ ) is ~190 nM and its fluorescence emission increases ~100-fold upon binding Ca<sup>2+</sup> with virtually no auto fluorescence [53]. Calcium Green-1 is also ~5-fold brighter than fluo-3 at saturating Ca<sup>2+</sup> levels [39]. Consequently, it can be used at 1/5 the concentration, which reduces problems with phototoxicity.

##### 4.2. Fluo-3

This dye has been one of the most popular and widely used Ca<sup>2+</sup> indicators. Because it is a single wavelength dye with fluorescein-like spectral characteristics, it can easily be excited with an argon laser (488 nm) for confocal microscopy or flow cytometry as well as with fluorescein filter sets in wide-field epi-fluorescent microscopes [41]. Its relatively lower Ca<sup>2+</sup> affinity ( $K_d$  ~ 390 nM) causes fewer problems with cytosolic buffering at resting Ca<sup>2+</sup> levels (~100 nM) when compared to Calcium Green-1. At rest and in the Ca<sup>2+</sup>-free form, fluorescence is minimal. However, its fluorescence increases over 100-fold when it binds Ca<sup>2+</sup>. As for other dyes, the  $K_d$  is sensitive to pH, protein binding, and temperature changes and should be measured *in vivo* for accurate Ca<sup>2+</sup> calibrations [54,55].

##### 4.3. Fluo-4

Fluo-4 is essentially a brighter, more photostable derivative of Fluo-3. Its Ca<sup>2+</sup> affinity is a little lower ( $K_d$  ~ 345 nM) and its absorption maximum is shifted ~12 nm compared to Fluo-3, making it more suitable for 488 excitation using an argon laser [43–45]. This makes Fluo-4 brighter at a lower dye concentration and consequently, less phototoxic. Lower concentrations of dye can yield almost double the amount of fluorescence, which is advantageous in cell lines plated at lower densities. As importantly, Fluo-4 has very low background absorbance and lower dye concentrations require shorter incubation times.

##### 4.4. Fura-2

This ratiometric dye is one of the most successful and popular Ca<sup>2+</sup> indicators and is widely considered the standard for quantitative intracellular Ca<sup>2+</sup> measurements (see below). Its peak absorbance shifts from 340 nm in the Ca<sup>2+</sup> bound state to 380 nm in the Ca<sup>2+</sup> free state. Fluorescence occurs at a peak wavelength of 500 nm for excitation at either UV wavelength. The primary disadvantage of Fura-2 is that it is a dual excitation dye and not suitable for confocal microscopy. Because of its UV excitation, it is also well

suitable for two-photon excitation albeit as a non-ratiometric indicator. Fura-2 has a Ca<sup>2+</sup> affinity ( $K_d$  ~ 145 nM) that is comparable to endogenous resting Ca<sup>2+</sup> levels [40,56]. It is relatively resistant to photobleaching but as with other indicator dyes, it can become compartmentalized [42,57,58]. Fura-2, as well as some of its lower affinity derivatives (Fura-2, namely Fura-4F, Fura-5F, Fura-6F, and Fura-FF) have wide sensitivity ranging from ~100 nM to ~100 μM. [59–62].

##### 4.5. Indo-1

This dye is also a well-known and widely used ratiometric Ca<sup>2+</sup> indicator. It differs from Fura-2 in that it is single excitation and dual emission. Peak absorption occurs in the UV at ~350 nm and peak emission occurs at ~405 and ~485 nm in the Ca<sup>2+</sup> bound and free states, respectively. Because it is single excitation, it is well suited for laser scanning microscopy. The primary disadvantage of Indo-1 is photo-instability [42]. Photobleaching can occur very rapidly, limiting its usefulness for confocal microscopy. However, it is still widely used for flow cytometry, where photo stability is less of an issue. The spectral properties of the dye have also been shown to work with three-photon excitation and unlike Fura-2, it retains its ratiometric emission [63]. It should be noted that the spectral properties of NADH autofluorescence overlap with those of Indo-1.

##### 4.6. Oregon Green 488 BAPTA

This dye has spectral characteristics that are similar to Fluo-3/4 and Calcium Green indicators. They are single excitation/emission dyes that are easily excited by an argon laser at 488 nm. The absorption peak is close to 488 nm and as with Calcium Green, the dye can be used at lower concentrations than Fluo-3/4, making it potentially less phototoxic [64]. The Ca<sup>2+</sup> affinity of Oregon Green 488 BAPTA-1 is relatively high ( $K_d$  ~ 170 nM), which can be advantageous for detecting small changes in Ca<sup>2+</sup> near resting levels. The Ca<sup>2+</sup> affinity of Oregon Green 488 BAPTA-2, which is a dimmer version of Oregon Green 488 BAPTA-1, is more comparable to Fluo-3 and Fluo-4 ( $K_d$  ~ 580 nM). The various derivatives of this class of indicators have a high quantum yield and have been used in microplate readers, a testament to their consistency [65,66]. Finally, Oregon Green 488 BAPTA absorbs two-photon excitation more efficiently than other fluorescein-like Ca<sup>2+</sup> indicators.

##### 4.7. Ca<sup>2+</sup> yellow, Ca<sup>2+</sup> orange, and Ca<sup>2+</sup> crimson

These single wavelength indicators are based on tetramethylrhodamine and Texas Red dyes with similar absorption/emission spectra. Ca<sup>2+</sup> affinities are relatively high ( $K_d$  ~ 170–185 nM). Ca<sup>2+</sup> crimson in particular has a very high excitation maximum, making it a good candidate for tissue with a lot of autofluorescence [67]. A major disadvantage of these rhodamine-like dyes is their tendency to rapidly compartmentalize [68,69]. In the case of Rhod-2 Ca<sup>2+</sup> indicator and its derivatives, this compartmentalization is preferentially restricted to the mitochondria and is discussed below in the section on low affinity Ca<sup>2+</sup> dyes.

##### 4.8. X-Rhod/Rhod-2

These single wavelength Ca<sup>2+</sup> dyes are also based on tetramethylrhodamine, with similar absorption/emission spectra. Peak absorption/emission wavelengths are ~557/581 nm for Rhod-2 and ~580/600 nm for X-Rhod-1, respectively. Unlike Ca<sup>2+</sup> orange and yellow, the Ca<sup>2+</sup> affinities are relatively low with  $K_d$ 's of ~570 and 700 nM for Rhod-2 and X-Rhod-1, respectively. Finally, the AM esters of these dyes have a net positive charge, which pro-

motes sequestration into mitochondria in many cells. The low affinity analogs of Rhod-2 and X-Rhod-1 (i.e. Rhod-5N, Rhod-FF and X-Rhod-5F, and X-Rhod-FF) are generally the preferred choices to measure  $\text{Ca}^{2+}$  levels in this energy generating organelle.

## 5. Low affinity $\text{Ca}^{2+}$ indicators

This class of indicators is frequently used to measure  $\text{Ca}^{2+}$  when very little buffering can be tolerated (albeit at the expense of signal strength) or in subcellular compartments where relatively high levels of intracellular  $\text{Ca}^{2+}$  are expected. For example, the optimal  $K_d$  for measuring  $\text{Ca}^{2+}$  in the endoplasmic reticulum (ER) is between 22 and 250  $\mu\text{M}$  given that the approximate ER concentration in most cells is in the range of 100–1000  $\mu\text{M}$  [70]. The procedures for loading these dyes for ER  $\text{Ca}^{2+}$  measurements vary slightly from the normal cytosolic loading procedures discussed above. Cells are incubated with AM-linked dyes as described for normal loading protocols, and allowing for additional incubation times as needed to also permit ER loading. Subsequent to general loading, the cytosol dye is unloaded either by plasma membrane permeabilization or for example, by diffusion into a patch-clamp pipette, to reveal the ER accumulated  $\text{Ca}^{2+}$  indicator [70]. A targeted-esterase induced dye loading (TED) technique has also been developed by Robert Blum's group [17]. Their approach technique is to trap low affinity  $\text{Ca}^{2+}$  indicators by targeting recombinant esterases into the ER. After stable expression of the ER-esterases, cells are incubated with the AM-linked  $\text{Ca}^{2+}$  indicator in the normal fashion [17]. In addition to the list previously described in Takahashi et al. [14], Molecular Probes offers many new dyes to use for  $\text{Ca}^{2+}$  measurements and are included in Table 3. Many of the low affinity  $\text{Ca}^{2+}$  indicators were originally designed for detection and measurement of magnesium (Mag) dynamics. Intracellular Mag concentrations remain relatively constant and hover around 1 mM. However, as a general rule, reagents that bind Mag also bind  $\text{Ca}^{2+}$  at  $\sim 4$ -fold higher affinity when compared to Mag binding (Table 3).

### 5.1. Mag-Fura-2

Previously known as Fura-2, Mag-Fura-2 is a  $\text{Mg}^{2+}/\text{Ca}^{2+}$  indicator widely used for intracellular measurements of these two divalent ions [60,71,72]. It is a ratiometric indicator. In the  $\text{Ca}^{2+}$  free form, Mag-Fura-2 has a peak excitation wavelength of 369 nm, whereas when  $\text{Ca}^{2+}$  is bound, the peak excitation wavelength is 329 nm. The peak emission wavelengths change little when Mag-Fura-2 is bound to  $\text{Ca}^{2+}$ ; changing from 511 to 508 nm when  $\text{Ca}^{2+}$  is bound. Mag-Fura-2 has a  $K_d$  of 1.9 mM for  $\text{Mg}^{2+}$  and a  $K_d$  of 25  $\mu\text{M}$  for  $\text{Ca}^{2+}$ . As mentioned above, the ion affinity for an indicator may vary depending on environmental conditions such as temperature, pH, ionic strength among others and the  $K_d$  obtained *in vivo* may be different from the one found *in vitro*. In general, the best conditions for imaging must be determined for each type of cell depending of the kind of measurements desired. For example, as mentioned by Golovina [77] primary cultured mouse astrocytes loaded with Mag-Fura-2 showed a typical cytosolic  $\text{Ca}^{2+}$  pattern when loaded at 22 °C. When the same conditions were used but temperature for loading the dye was changed to 36 °C the cells showed a distinct ER  $\text{Ca}^{2+}$  pattern, which remain even after permeabilization with saponin.

### 5.2. Mag-Fluo-4

Mag-Fluo-4 is a single wavelength excitation/emission indicator. It has a  $K_d$  for  $\text{Ca}^{2+}$  of 22  $\mu\text{M}$  and for  $\text{Mg}^{2+}$  of 4.7 mM. The excitation peak for this indicator is at 490 nm with an emission

at 517 nm. To visualize this indicator, most investigators use a 488 excitation (argon ion laser source) and a 505–550 emission filter. A FITC filter cube in a conventional wide-field microscope also works well. Mag-Fluo-4 is essentially non-fluorescent in the absence of divalent cations and it increases its fluorescence upon binding  $\text{Ca}^{2+}$  [53].

### 5.3. Mag-Indo-1

Like Mag-Fura-2, Mag-Indo-1 is another type of ratiometric  $\text{Mg}^{2+}/\text{Ca}^{2+}$  indicator. Its excitation wavelength is  $\sim 350$  nm and the fluorescence is monitored between 390 and 480, which are the peaks emission wavelengths for the  $\text{Ca}^{2+}$  bound and  $\text{Ca}^{2+}$  free forms of this indicator. It has a  $K_d$  for  $\text{Ca}^{2+}$  of 35  $\mu\text{M}$  and for  $\text{Mg}^{2+}$  of 2.7  $\mu\text{M}$ .

### 5.4. Mag-Fura-5

It has a  $K_d$  of 28  $\mu\text{M}$ . It has been successfully used to monitor  $\text{Ca}^{2+}$  dynamics in isolated mammalian skeletal muscle fibers [93,94] and mouse motor neurons of the spinal cord [75] among other cell types.

### 5.5. Mag-Fura-Red

This dye has a  $K_d$  of 17  $\mu\text{M}$ . It has been used to detect light-induced  $\text{Ca}^{2+}$  release from the ER in permeabilized photoreceptors from invertebrates [76].

### 5.6. Fura-2-FF

This  $\text{Ca}^{2+}$  indicator has a  $K_d$  of 35  $\mu\text{M}$  and is ratiometric. It has been successfully used in skeletal muscle fibers [95].

### 5.7. Fluo-5N

This dye is a low affinity single wavelength  $\text{Ca}^{2+}$  indicator with a  $K_d$  of 90  $\mu\text{M}$ . It has been used in a wide range of cells including cardiac myocytes [96], pulmonary arterial smooth muscle cells [97], and lobster hepatopancreas [98].

### 5.8. Oregon Green BAPTA-5N

Oregon Green BAPTA-5N is an indicator with a  $K_d$  of 20  $\mu\text{M}$ . It has been used to measure  $\text{Ca}^{2+}$  in photoreceptors of invertebrates [99], gastric myocytes [80], cardiac myocytes [100], skeletal muscle fibers [101].

### 5.9. Rhod-5N, Rhod-FF and X-Rhod-5F, and X-Rhod-FF

These dyes are low affinity derivatives of Rhod-2 and X-Rhod-1. The  $K_d$ s are 19 and 320  $\mu\text{M}$  for Rhod-5N and Rhod-FF, respectively. The  $K_d$ s for X-Rhod-5F and X-Rhod-FF are 1.6 and 17  $\mu\text{M}$ , respectively. The peak emission wavelength of X-Rhod derivatives are also red-shifted to  $\sim 600$  nm [53].

## 6. Calibrating the fluorescence of chemical $\text{Ca}^{2+}$ indicators

Several procedures are used to either normalize or calibrate the fluorescence signals of  $\text{Ca}^{2+}$  dyes. When absolute values are not required, a simple normalization procedure is utilized to compare the relative fluorescent signals between experiments. For single wavelength excitation/emission dyes, the simplest procedure is to divide changes in the fluorescent signal by the average resting fluorescence according to the formula:

$$\Delta\text{Ca}^{2+} = \Delta F/F = (F - F_{\text{rest}})/F_{\text{rest}} \quad (3)$$

where  $F$  is the dye fluorescence at any given time and  $F_{\text{rest}}$  is the average fluorescence signal prior to an experimental manipulation (e.g. addition of an agonist). This formulization is easy, rapid and excellent for studying changes in  $\text{Ca}^{2+}$  between experiments, but at the expense of eliminating information on the resting levels of  $\text{Ca}^{2+}$ . Ratiometric dyes are required when the user is interested in comparing the resting fluorescent signals between experiments. In this case, the simplest procedure is to divide the intensity of the fluorescent signals in the  $\text{Ca}^{2+}$  bound ( $F_{\text{Ca-bound}}$ ) and  $\text{Ca}^{2+}$  free ( $F_{\text{Ca-free}}$ ) states of the dye according to the following formula:

$$\Delta\text{Ca}^{2+} = F_{\text{Ca-bound}}/F_{\text{Ca-free}} \quad (4)$$

For Fura-2,  $F_{\text{Ca-bound}}$  refers to the fluorescent intensity at  $\sim 500$  nm when the dye is excited at 340 nm and  $F_{\text{Ca-free}}$  (also at  $\sim 500$  nm) when the dye is excited at 380 nm. For Indo-1, a single wavelength of excitation is used ( $\sim 350$  nm) and  $F_{\text{Ca-bound}}$  refers to the fluorescent intensity at  $\sim 405$  nm and  $F_{\text{Ca-free}}$  is the fluorescent intensity at  $\sim 485$  nm.

Standard  $\text{Ca}^{2+}$  calibration procedures need to be performed when estimates of the absolute level of  $\text{Ca}^{2+}$  are required. For single wavelength indicators, the following calibration formula is generally used:

$$[\text{Ca}^{2+}] = K_d[(F - F_{\text{min}})/(F_{\text{max}} - F)] \quad (5)$$

where  $K_d$  is the dissociation constant of the dye,  $F$  is the fluorescence value obtained at any time during the recording,  $F_{\text{min}}$  is the fluorescence in the absence of  $\text{Ca}^{2+}$  and  $F_{\text{max}}$  is the fluorescence at saturating  $[\text{Ca}^{2+}]$  [47].  $F_{\text{min}}$  and  $F_{\text{max}}$  are empirically determined in approximately zero and saturating  $\text{Ca}^{2+}$  environments using permeabilized cells as carefully described elsewhere [14]. The  $K_d$  can be estimated by systematically increasing the concentration of  $\text{Ca}^{2+}$  and determining the level at which half-maximal fluorescence intensity is reached. It is usually not necessary to determine the  $K_d$  for each experimental series. However,  $F_{\text{min}}$  and  $F_{\text{max}}$  need to be estimated for each cell of interest because of their dependence on the dye concentration.

The calibration procedure for ratiometric dyes generally proceeds from the classic formula originally published by Roger Tsien's group [47]. Accordingly,

$$[\text{Ca}^{2+}] = K_d(S_{f2}/S_{b2})(R - R_{\text{min}})/(R_{\text{max}} - R) \quad (6)$$

where the  $K_d$  is the dissociation constant of the dye,  $S_{f2}$  is the maximum fluorescence intensity for zero  $\text{Ca}^{2+}$  obtained at the wavelength used to monitor free  $\text{Ca}^{2+}$ ,  $S_{b2}$  is the minimum fluorescence intensity at saturating  $\text{Ca}^{2+}$  (obtained with the same wavelength as  $S_{f2}$ ), and  $R_{\text{min}}$  and  $R_{\text{max}}$  are the fluorescence ratio values obtained at conditions of zero  $\text{Ca}^{2+}$  and at saturating  $\text{Ca}^{2+}$ , respectively [47,102,103]. As noted above, accurate calibrations require that the  $K_d$  be determined *in situ*, but not necessarily for each experiment. Procedures to calibrate fluorescent signals in organelles, e.g. the ER or mitochondrial, are essentially identical [102].

## 7. In vivo $\text{Ca}^{2+}$ -imaging

Recent technical advances have permitted single cell  $\text{Ca}^{2+}$  signaling to be performed *in vivo* (for reviews, see Refs. [67,109]). In this section, we review our laboratory procedures for  $\text{Ca}^{2+}$  imaging in the cortex of living mice. With relatively minor changes, similar approaches should also permit live  $\text{Ca}^{2+}$  signals to be imaged in other tissues. We have used both confocal and two-photon microscopy for these *in vivo* measurements. The former excitation system has the advantage that the single wavelength fluorescein-like  $\text{Ca}^{2+}$  indicators can be efficiently excited, which are much brighter than when excited by two-photon lasers. Single photon absorption curves are also relatively narrow compared to two-photon absorp-

tion curves for the same  $\text{Ca}^{2+}$  indicators, which makes it much more practical to excite individual dyes one at a time. The primary advantage of two-photon absorption strategies for  $\text{Ca}^{2+}$  indicators are less phototoxicity, as well as, less light scatter, which permits imaging in thick tissues to much greater depths.

Strong loading of  $\text{Ca}^{2+}$  dyes is critical for any experiment, but especially so for *in vivo* recordings. There are several options available, including the well-established dye injection techniques utilizing microelectrodes, which can also be configured for electrophysiological recordings, or with pressure ejection-based local dye delivery. Examples of these approaches have recently been published for the mammalian brain [104–106] and for the zebrafish spinal cord [107]. However, single cell dye injections are labor intensive and severely limit the number of cells that can be recorded from. Fortunately, a simpler procedure for loading cortical astrocytes has now been discovered.

### 7.1. Cortical loading of $\text{Ca}^{2+}$ indicator dyes

#### 7.1.1. Surgical preparation

The first step in any live animal imaging experiment is to anesthetize the animal. It has been our experience that the choice of anesthetic plays a critical role in the ability of the dyes to load into cortical astrocytes (unpublished observations). The deeper the anesthesia, the more problematic the loading of the dyes can become. The underlying reason for this is currently unknown, but presumably relates to the inactivation of transmembrane transport processes during times of hypoxia. Our laboratory has experimented with two different anesthetics (urethane and isoflurane) and found a similar affect on dye loading. When using urethane, which is the easiest to implement, all that is required are small, sequential IP injections of anesthetic, so that the depth of anesthesia can be carefully titrated. In total, we administer  $\sim 70$  mg/kg chloralose and 700 mg/kg urethane for each mice. The disadvantage of urethane is that it is easy to overshoot the level of anesthesia and it is also difficult for mice to recover. Consequently, we reserve the use of urethane anesthesia for terminal experiments. The use of isoflurane as an anesthetic requires a precision vaporizer for delivery, which can be purchased for  $\sim \$1500$ – $\$2000$  from a number of companies, as well as a ventilator ( $\sim \$3300$  Minivent, Harvard Apparatus). Dye loading is generally sufficient when our mice are kept anesthetized at 0.6–0.9% isoflurane and body temperature is maintained, with a simple heating pad maintained, at  $37^\circ\text{C}$ . We maintain the respiratory rate of animals at  $\sim 100$  breaths/min (measured using the MouseOx system, STARR Life Sciences Corporation,  $\sim \$4500$ ).

### 7.2. Loading $\text{Ca}^{2+}$ dyes into cortical astrocytes

Once the animal is sufficiently anesthetized (as determined by paw pinch), the cranial hair is shaved and an incision is made in the scalp. The exposed skull is then cleaned and a custom made stainless steel ring is glued (VetBond, 3 M) to a flat region of bone overlying the parietal cortex (between  $-1$  to  $-3$  mm post-bregma and 2 to 4 mm lateral) (Fig 1). The ring is fixed to a stereotaxic frame to help insure that the animal remains stationary during the remaining procedures, as well as during data image collection. At this time, we also apply a small amount of low melting agar to seal the contact region between the stainless steel ring and bone, so that fluids do not leak. A small 1–2 mm hole is drilled through the cranium using a high-speed dremel-like tool (MH-01 Hammer Handpiece with the HP4-91 Controller, Foredom Electric Company). Drilling and manual removal of the dura are preformed with a micro-tipped needle (Fine Science Tools, No. 26007-02, to create an initial tear in the dura) and fine tipped forceps (0.01 mm, Dumont, Fine Science Tools) under artificial cerebral fluid (ASF) using



**Fig. 1.** Optical Imaging *in vivo* of the mouse parietal cortex. Left panel shows the objective inverter attached to a Zeiss LSM 510 multiphoton microscope positioning the 60× 1.1 NA water immersion objective above the mouse parietal cortex. Right panel is a higher magnification of the stainless steel ring holder that is glued to the skull and immobilizes the brain. The center ring has been filled with 2% agarose (Sigma type VII) and sealed from above with a glass coverslip (#0). This essentially eliminates motion artifacts due to breathing when the hole in the cranium is less than 1–2 mm in diameter. The red heating pad is maintained at 37 °C.

a surgical grade dissecting scope (Nikon SMZ1500). With care, the surface of the cortex can easily be exposed without damaging the cortex. Imaging dyes are then pipetted on the surface of the cortex for ~30–60 min, depending on the dye. The surface is washed and the cranium hole sealed by filling it with 2% agarose (Agarose, Type

VII, low melting temperature; Sigma) and by gently capping the stainless steel ring with a glass coverslip (#0). The sandwiched agarose helps to dampen movement of the tissue due to respiration of the mouse. The agarose plug can be subsequently removed and replaced with a new plug after adding and/or injecting reagents.

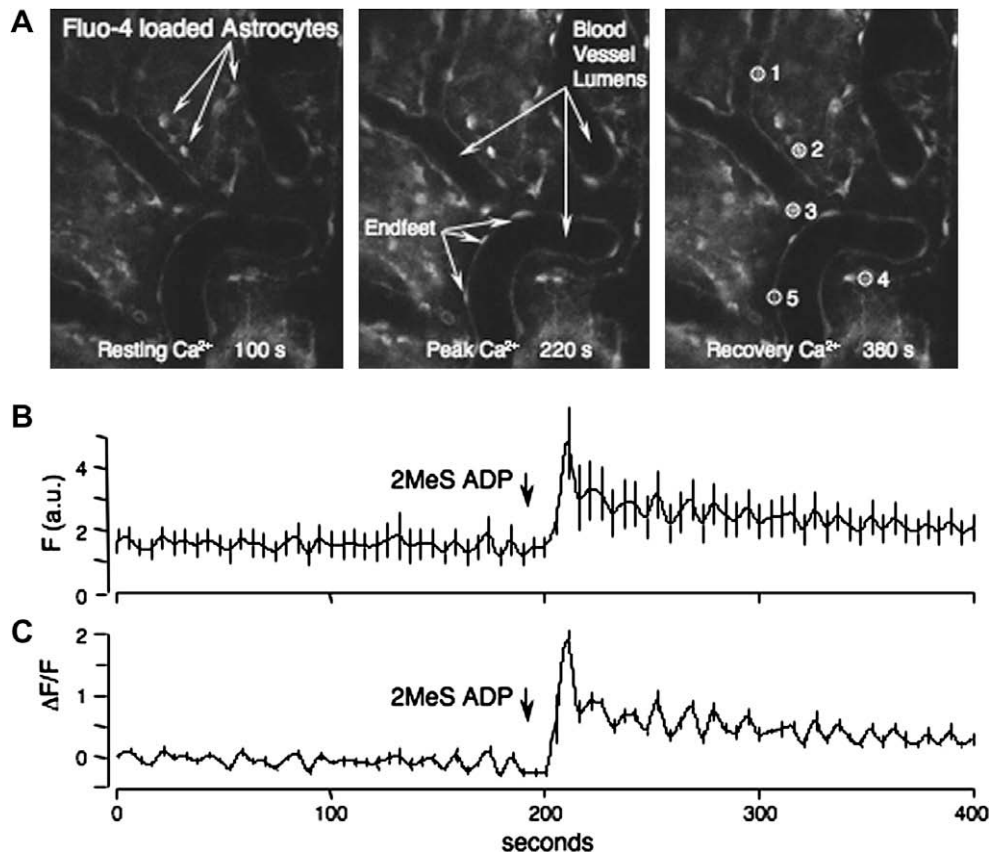


**Fig. 2.** *In vivo*  $\text{Ca}^{2+}$  imaging in mouse cortical astrocytes using Fluo-4 AM. A mouse was anesthetized with isoflurane and the cortex prepared as described in the text. Fluo-4 AM (50  $\mu\text{g}$ ) was vortexed with 5  $\mu\text{l}$  Pluronic F-127, mixed with ASF to a final concentration of 100  $\mu\text{M}$  and pipetted onto the cortical surface for ~60 min. (A) *In vivo* images of the mouse cortex loaded with Fluo-4 AM at the three time points as labeled. Images were collected on a Nikon C1si confocal microscope fitted with an objective inverter with a 40X objective. A time course of Fluo-4 fluorescence was collected with images acquired every 5 seconds. Resting levels of  $\text{Ca}^{2+}$  were imaged (left panel) before the P2Y1R agonist, 2MeS ADP (100  $\mu\text{M}$ ), was added to the cortex. The middle panel shows the peak Fluo-4 fluorescence in response to 2MeS ADP. The right panel shows the recovery of the cells from 2MeS ADP (380 s). (B) Lineplot of the averaged fluorescence intensity (F) of the five individual cells identified in the right panel of (A). (C) Graph of the same data in (B), but plotted as  $\Delta F/F$  using the formula  $(F - \text{Frest})/\text{Frest}$ . Note the smaller standard error compared to that in (B). Data was analyzed using Image J.

The mouse is then ready for imaging. Because our microscope system is inverted, we purchased an objective inverted from LSM Technologies, Incorporated. This adaptor permits *in vivo* imaging on conventional, confocal and two-photon microscopes (see Fig. 1).

An example of  $\text{Ca}^{2+}$ -imaging using the procedure described above is presented in Fig. 2. Changes in the fluorescence of Fluo-4 AM in response to a purinergic receptor agonist (2meSADP) added to the cortex are shown. Five cells were analyzed using ImageJ for fluorescent change overtime and the average of these cells are depicted in two graphs. The first graph shows the average fluorescence in raw format (Fig. 2B), while the second graph (Fig. 2C) depicts the same cells changes in  $\text{Ca}^{2+}$  using Eq. 2 described above. Note the difference in the size of the standard error bars between the two graphs presented in Fig. 2. Using the equation allows one to correct for the variation between cells in basal fluorescence units and tightens the standard error.

The strength and depth of penetration of the dyes depends on several factors including the health status of the animal, the depth of anesthesia, and on the length of time the dye is allowed to remain on the brain. Body temperature and if possible, pH of the animal should be monitored and maintained at physiological levels (36–37 °C) [108]. In our experience when utilizing confocal microscopy the imaging depth can range between 100 and 150  $\mu\text{m}$  and with two-photon microscopy to a depth of over 500  $\mu\text{m}$  (typically, 300–400  $\mu\text{m}$ ).

It has also been demonstrated that the *in vivo* dye loading procedure described above primarily loads astrocytes. This has been achieved through labeling cells with both SR101 (an astrocyte specific marker) in conjunction with Fluo-4 AM. There is a large overlap in the staining of astrocytes with Fluo-4 AM [104].

## 8. Conclusion

In conclusion, the most common chemical  $\text{Ca}^{2+}$  indicators used for the investigation of intracellular  $\text{Ca}^{2+}$  signaling have been presented along with relevant methodologies. As we described in the text there are a number of characteristics for each dye that must be considered by the enduser to obtain relevant data. One of the greatest advances since our last review is that of *in vivo*  $\text{Ca}^{2+}$  imaging. This technique will likely become increasingly utilized as the methodology is improved.

## References

- [1] M.J. Berridge, *Nature* 361 (1993) 315–325.
- [2] U. Wojda, E. Salinska, J. Kuznicki, *IUBMB Life* 60 (2008) 575–590.
- [3] P. Nicotera, S. Orrenius, *Cell Calcium* 23 (1998) 173–180.
- [4] M.P. Mattson, *Aging Cell* 6 (2007) 337–350.
- [5] D.H. MacLennan, *Eur. J. Biochem.* 267 (2000) 5291–5297.
- [6] M. Periasamy, A. Kalyanasundaram, *Muscle Nerve* 35 (2007) 430–442.
- [7] E.G. Kranias, D.M. Bers, *Subcell Biochem.* 45 (2007) 523–537.
- [8] S.E. Lehnart, *Curr. Opin. Pharmacol.* 7 (2007) 225–232.
- [9] B. Pani, B.B. Singh, *Cell Mol. Life Sci.* 65 (2008) 205–211.
- [10] L. Missiaen, W. Robberecht, L.V. Bosch, G. Callewaert, J.B. Parys, F. Wuytack, L. Raeymaekers, B. Nilius, J. Eggermont, H.D. Smedt, *Cell Calcium* 28 (2000) 1–21.
- [11] H.L. Roderick, J.D. Lechleiter, P. Camacho, *J. Cell Biol.* 149 (2000) 1235–1248.
- [12] Y. Li, P. Camacho, *J. Cell Biol.* 164 (2004) 35–46.
- [13] L. Raeymaekers, *Cell Calcium* 23 (1998) 261–268.
- [14] A. Takahashi, P. Camacho, J.D. Lechleiter, B. Herman, *Physiol. Rev.* 79 (1999) 1089–1125.
- [15] Invitrogen, <http://www.invitrogen.com/>.
- [16] A.E. Palmer, R.Y. Tsien, *Nat. Protoc.* 1 (2006) 1057–1065.
- [17] M. Rehberg, A. Lepier, B. Solchenberger, P. Osten, R. Blum, *Cell Calcium* 44 (2008) 386–399.
- [18] R.C. Rogers, J.S. Nasse, G.E. Hermann, *J. Neurosci. Methods* 150 (2006) 47–58.
- [19] A.C. Kreitzer, K.R. Gee, E.A. Archer, W.G. Regehr, *Neuron* 27 (2000) 25–32.
- [20] J. Shuai, I. Parker, *Cell Calcium* 37 (2005) 283–299.
- [21] S. Prilloff, M.I. Noblejas, V. Chedhomme, B.A. Sabel, *Eur. J. Neurosci.* 25 (2007) 3339–3346.
- [22] P. Jezek, J. Hanus, C. Semrad, K. Garlid, *J. Biol. Chem.* 271 (1996) 6199–6205.
- [23] M.L. Woodruff, A.P. Sampath, H.R. Matthews, N.V. Krasnoperova, J. Lem, G.L. Fain, *J. Physiol.* 542 (2002) 843–854.
- [24] A.E. Oliver, G.A. Baker, R.D. Fugate, F. Tablin, J.H. Crowe, *Biophys. J.* 78 (2000) 2116–2126.
- [25] D. Larsson, B. Larsson, T. Lundgren, K. Sundell, *Anal. Biochem.* 273 (1999) 60–65.
- [26] F.A. Lattanzio Jr., *Biochem Biophys Res Commun* 171 (1990) 102–108.
- [27] J.P. Kao, R.Y. Tsien, *J. Biophys.* 53 (1988) 635–639.
- [28] M.G. Klein, B.J. Simon, G. Szucs, M.F. Schneider, *J. Biophys.* 53 (1988) 971–988.
- [29] S.M. Baylor, S. Hollingworth, *J. Physiol.* 403 (1988) 151–192.
- [30] R.P. Haugland, *Handbook of fluorescent probes and research chemicals*, Molecular Probes, Eugene, OR, 1996.
- [31] M. Zhao, S. Hollingworth, S.M. Baylor, *Biophys. J.* 70 (1996) 896–916.
- [32] P. Lipp, C. Luscher, E. Niggli, *Cell Calcium* 19 (1996) 255–266.
- [33] R.A. Floto, M.P. Mahaut-Smith, B. Somasundaram, J.M. Allen, *Cell Calcium* 18 (1995) 377–389.
- [34] P. Nicotera, A.D. Rossi, *Mol. Cell. Biochem.* 135 (1994) 89–98.
- [35] D. Schild, A. Jung, H.A. Schultens, *Cell Calcium* 15 (1994) 341–348.
- [36] P. Lipp, E. Niggli, *Cell Calcium* 14 (1993) 359–372.
- [37] C.Y. Okada, M. Rechsteiner, *Cell* 29 (1982) 33–41.
- [38] J.P. Kao, *Methods Cell Biol* 40 (1994) 155–181.
- [39] M. Eberhard, P. Erne, *Biochem. Biophys. Res. Comm.* 180 (1991) 209–215.
- [40] T.W. Hurley, M.P. Ryan, R.W. Brinck, *Am. J. Physiol.* 263 (1992) C300–C307.
- [41] J.P. Kao, A.T. Harootyanian, R.Y. Tsien, *J. Biol. Chem.* 264 (1989) 8179–8184.
- [42] M. Wahl, M.J. Lucherini, E. Gruenstein, *Cell Calcium* 11 (1990) 487–500.
- [43] K.R. Gee, K.A. Brown, W.N. Chen, J. Bishop-Stewart, D. Gray, I. Johnson, *Cell Calcium* 27 (2000) 97–106.
- [44] V.A. Miriel, J.R. Mauban, M.P. Blaustein, W.G. Wier, *J. Physiol.* 518 (Pt. 3) (1999) 815–824.
- [45] J. Chambers, R.S. Ames, D. Bergsma, A. Muir, L.R. Fitzgerald, G. Hervieu, G.M. Dytko, J.J. Foley, J. Martin, W.S. Liu, J. Park, C. Ellis, S. Ganguly, S. Konchar, J. Cluderay, R. Leslie, S. Wilson, H.M. Sarau, *Nature* 400 (1999) 261–265.
- [46] E.F. Etter, A. Minta, M. Poenie, F.S. Fay, *Proc. Natl. Acad. Sci. USA* 93 (1996) 5368–5373.
- [47] G. Grynkiewicz, M. Poenie, R.Y. Tsien, *J. Biol. Chem.* 260 (1985) 3440–3450.
- [48] K.L. Brain, M.R. Bennett, *J. Physiol.* 502 (Pt 3) (1997) 521–536.
- [49] D.L. Wokosin, C.M. Loughrey, G.L. Smith, *Biophys. J.* 86 (2004) 1726–1738.
- [50] J.C. Mercer, W.I. Dehaven, J.T. Smyth, B. Wedel, R.R. Boyles, G.S. Bird, J.W. Putney Jr., *J. Biol. Chem.* 281 (2006) 24979–24990.
- [51] I. Micu, A. Ridsdale, L. Zhang, J. Woulfe, J. McClintock, C.A. Brantner, S.B. Andrews, P.K. Stys, *Nat. Med.* 13 (2007) 874–879.
- [52] L.E. Garcia-Chacon, K.T. Nguyen, G. David, E.F. Barrett, *J. Physiol.* 574 (2006) 663–675.
- [53] <<http://probes.invitrogen.com/handbook/sections/1903.html>>.
- [54] D. Thomas, S.C. Tovey, T.J. Collins, M.D. Bootman, M.J. Berridge, P. Lipp, *Cell Calcium* 28 (2000) 213–223.
- [55] C. Perez-Terzic, M. Jaconi, D.E. Clapham, *Bioessays* 19 (1997) 787–792.
- [56] J. Pesco, J.M. Salmon, J. Vigo, P. Viallet, *Anal. Biochem.* 290 (2001) 221–231.
- [57] W.J. Scheenen, L.R. Makings, L.R. Gross, T. Pozzan, R.Y. Tsien, *Chem. Biol.* 3 (1996) 765–774.
- [58] P.L. Becker, F.S. Fay, *Am. J. Physiol.* 253 (1987) C613–C618.
- [59] D. Ogden, K. Khodakhah, T. Carter, M. Thomas, T. Capiod, *Pflugers Arch.* 429 (1995) 587–591.
- [60] A.M. Hofer, I. Schulz, *Cell Calcium* 20 (1996) 235–242.
- [61] E. Neher, *Exp. Brain Res. Ser.* 14 (1986) 80–96.
- [62] K.R. Gee, E.A. Archer, L.A. Lapham, M.E. Leonard, Z.L. Zhou, J. Bingham, Z. Diwu, *Bioorg. Med. Chem. Lett.* 10 (2000) 1515–1518.
- [63] H. Szmajkowski, I. Gryczynski, J.R. Lakowicz, *Biophys. J.* 70 (1996) 547–555.
- [64] K. Svoboda, W. Denk, D. Kleinfeld, D.W. Tank, *Nature* 385 (1997) 161–165.
- [65] M.U. Kassack, B. Hofgen, J. Lehmann, N. Eckstein, J.M. Quillan, W. Sadee, *J. Biomol. Screen.* 7 (2002) 233–246.
- [66] K. Lin, W. Sadee, J.M. Quillan *Biotechniques* 26 (1999) 318–322, 324–326.
- [67] S. Duffly, B.A. MacVicar, *J. Neurosci.* 15 (1995) 5535–5550.
- [68] P.J. Del Nido, P. Glynn, P. Buenaventura, G. Salama, A.P. Koretsky, *Am. J. Physiol.* 274 (1998) H728–H741.
- [69] F.J. Richmond, R. Gladdy, J.L. Creasy, S. Kitamura, E. Smits, D.B. Thomson, *J. Neurosci. Methods* 53 (1994) 35–46.
- [70] M.K. Park, A.V. Tepikin, O.H. Petersen, *Pflugers Arch.* 444 (2002) 305–316.
- [71] A.M. Hofer, W.R. Schlue, S. Curci, T.E. Machen, *FASEB J.* 9 (1995) 788–798.
- [72] A.M. Hofer, C. Fasolato, T. Pozzan, *J. Cell Biol.* 140 (1998) 325–334.
- [73] M.K. Park, O.H. Petersen, A.V. Tepikin, *EMBO J.* 19 (2000) 5729–5739.
- [74] B.S. Launikonis, J. Zhou, L. Royer, T.R. Shannon, G. Brum, E. Rios, *J. Physiol.* 567 (2005) 523–543.
- [75] J. Palecek, M.B. Lips, B.U. Keller *J. Physiol.* 520 (Pt. 2) (1999) 485–502.
- [76] K. Ukhanov, S.J. Mills, B.V. Potter, B. Walz, *Cell Calcium* 29 (2001) 335–345.
- [77] V.A. Golovina, M.P. Blaustein, *Science* 275 (1997) 1643–1648.
- [78] M.J. Deviney 2nd, I.J. Reynolds, K.E. Dineley, *Cell Calcium* 37 (2005) 225–232.
- [79] D.X. Brochet, D. Yang, A. Di Maio, W.J. Lederer, C. Franzini-Armstrong, H. Cheng, *Proc. Natl. Acad. Sci. USA* 102 (2005) 3099–3104.
- [80] C. White, G. McGeown, *Cell Calcium* 31 (2002) 151–159.
- [81] H. Shirakawa, S. Miyazaki, *Biophys. J.* 86 (2004) 1739–1752.
- [82] S. Patel, L.D. Gaspers, S. Boucherie, E. Memin, K.A. Stellato, G. Guillon, L. Combettes, A.P. Thomas, *J. Biol. Chem.* 277 (2002) 33776–33782.
- [83] S.L. Mironov, M.V. Ivannikov, M. Johansson, *J. Biol. Chem.* 280 (2005) 715–721.



- [84] J. Casas, M.A. Gijon, A.G. Vigo, M.S. Crespo, J. Balsinde, M.A. Balboa, J. Biol. Chem. 281 (2006) 6106–6116.
- [85] D. Zenisek, V. Davila, L. Wan, W. Almers, J. Neurosci. 23 (2003) 2538–2548.
- [86] H.F. Altimimi, P.P. Schnetkamp, J. Biol. Chem. 282 (2007) 3720–3729.
- [87] H. Daniel, A. Rancillac, F. Crepel, J. Physiol. 557 (2004) 159–174.
- [88] K. Tanaka, L. Khiroug, F. Santamaria, T. Doi, H. Ogasawara, G.C. Ellis-Davies, M. Kawato, G.J. Augustine, Neuron 54 (2007) 787–800.
- [89] I.V. Peshenko, A.M. Dizhoor, J. Biol. Chem. 281 (2006) 23830–23841.
- [90] W. Coatesworth, S. Bolsover, Cell Calcium 39 (2006) 217–225.
- [91] J.I. Bruce, D.R. Giovannucci, G. Blinder, T.J. Shuttleworth, D.I. Yule, J. Biol. Chem. 279 (2004) 12909–12917.
- [92] K.M. Marks, M. Rosinov, G.P. Nolan, Chem. Biol. 11 (2004) 347–356.
- [93] P. Szentesi, V. Jacquemond, L. Kovacs, L. Csernoch, J. Physiol. 505 (Pt. 2) (1997) 371–384.
- [94] O. Delbono, E. Stefani, J. Physiol. 463 (1993) 689–707.
- [95] D. Ursu, R.P. Schuhmeier, W. Melzer, J. Physiol. 562 (2005) 347–365.
- [96] X. Wu, D.M. Bers, Circ. Res. 99 (2006) 283–291.
- [97] X.R. Yang, M.J. Lin, K.P. Yip, L.H. Jeyakumar, S. Fleischer, G.P. Leung, J.S. Sham, Am. J. Physiol. Lung Cell Mol. Physiol. 289 (2005) L338–L348.
- [98] P. Chavez-Crooker, P. Pozo, H. Castro, M.S. Dice, I. Boutet, A. Tanguy, D. Moraga, G.A. Ahearn, Comp. Biochem. Physiol. C Toxicol. Pharmacol. 136 (2003) 213–224.
- [99] R. Payne, J. Demas, J. Gen. Physiol. 115 (2000) 735–748.
- [100] J.S. Fan, P. Palade, J. Physiol. 516 (Pt. 3) (1999) 769–780.
- [101] M. DiFranco, D. Novo, J.L. Vergara, Pflugers Arch. 443 (2002) 508–519.
- [102] A.M. Hofer, Methods Mol. Biol. 312 (2006) 229–247.
- [103] A.J. Morgan, A.P. Thomas, Methods Mol. Biol. 312 (2006) 87–117.
- [104] A. Nimmerjahn, F. Kirchhoff, J.N. Kerr, F. Helmchen, Nat. Methods 1 (2004) 31–37.
- [105] K. Ohki, S. Chung, Y.H. Ch'ng, P. Kara, R.C. Reid, Proc. Natl. Acad. Sci. USA 102 (2005) 597–603.
- [106] C. Stosiek, O. Garaschuk, K. Holthoff, A. Konnerth, Proc. Natl. Acad. Sci. USA 100 (2003) 7319–7324.
- [107] E. Brustein, N. Marandi, Y. Kovalchuk, P. Drapeau, A. Konnerth, Pflugers Arch. 446 (2003) 766–773.
- [108] The UFAW Handbook on the Care & Management of Laboratory Animals, sixth ed, Longman Scientific & Technical, England, 1986.
- [109] F. Helmchen, J. Waters, Eur. J. Pharmacol. 447 (2002) 119–129.